

# **EXTRACTION OF ALUMINA FROM KAOLIN FOUND IN GEM MINING SITES OF SRI LANKA**

## **ABSTRACT**

Kaolinitic clay deposits, esteemed as valuable mineral resources in Sri Lanka, are widely distributed throughout the country. Clay deposits in the Ratnapura District are often unearthed during gem mining operations. Unfortunately, excavated deposits are frequently disposed of openly on the ground without undergoing any value-addition process. This practice alters the soil condition of the vicinity, as the clay soil blocks the gravitational flow of rainwater. This environmental impact can be overcome by adding commercial value to these kaolinitic clay deposits. The present study aims to demonstrate the feasibility of extracting alumina from kaolinitic clay found at gem mining sites and to evaluate the potential of the extracted alumina as an adsorbent. Kaolinitic clay samples were collected from a gem mining site in the Ratnapura District. First, kaolin was transformed into metakaolin through calcination, and then alumina was extracted from the metakaolin via acid leaching using HCl as the leaching agent. Aluminum ions were separated from the leaching solution as  $\text{Al}(\text{OH})_3$  using NaOH as the precipitant. The precipitated  $\text{Al}(\text{OH})_3$  was transformed into alumina by calcination. The adsorption properties of the extracted alumina were evaluated using methylene blue solution as the adsorbate. Kaolin, extracted, and commercial alumina samples were characterized using XRD, XRF, FTIR, and SEM analysis. XRF analysis revealed that kaolin consists of 29.11% alumina by weight, and the purity of the extracted alumina was 90.03%. The crystalline phase of extracted alumina was identified as the  $\gamma$  phase via XRD analysis. Extracted and commercial alumina exhibited similar trends in the adsorption of methylene blue under varying adsorption parameters. **Accordingly,  $\gamma$ -phase alumina with a purity exceeding 90% can be produced from the kaolinitic clay found at the gem mining site under these experimental conditions. The extracted alumina has demonstrated potential for use as an adsorbent, exhibiting compatibility with commercial alumina.**

*Keywords: Alumina, Kaolin, Calcination, Acid leaching, Adsorbent, Adsorption*

## **1. INTRODUCTION**

Aluminum oxide, commonly known as alumina, is the only oxide of aluminum. Alumina possesses a crystalline structure that exhibits multiple polymorphic phases, including  $\alpha$ ,  $\beta$ ,  $\gamma$ ,  $\delta$ ,  $\theta$ ,  $\eta$ ,  $\kappa$ ,  $\chi$ , and  $\rho$  [1]. Each alumina phase displays differences in physicochemical properties, leading to its versatile industrial applications [2]. Alumina is widely utilized as catalysts, catalytic supports, abrasive, and adsorbents [3,4]. Alumina is preferred as an adsorbent due to its thermal and chemical stability, easy usage, and low cost [5,6]. The  $\gamma$ -phase alumina is primarily utilized as an adsorbent because of its high surface area and porosity characteristics [5].

Bauxite is the principal ore for alumina, and the Bayer Process is the predominant commercial method for alumina production [4,7]. The Bayer process requires high-grade bauxite, containing no more than 7% silica [8]. The processing of low-grade bauxite is considered uneconomical due to the loss of alumina and soda [9]. High-grade bauxite deposits are rare; most have already been exploited for aluminum production [9]. Non-bauxite minerals, such as clay, mica, shales, coal gangue, alunite, and fly ash, have been investigated as alternative sources for alumina production [10,11].

Clays are aluminosilicates with traces of alkali-metal and iron oxides, offering robust alternatives for alumina production as abundant and low-cost raw materials [12]. Among various types of clay, kaolin has the highest alumina content, typically ranging from 20% to 40%, making it the most suitable

candidate for alumina production [13]. In Sri Lanka, most clay deposits primarily consist of kaolin, containing up to 35% alumina. Kaolin deposits in the Ratnapura District are often excavated during gem mining operations. However, these deposits havenot undergone any value-addition process and are frequently openly dumped on the ground. Consequently, these kaolin deposits alter the soil condition in the vicinity by primarily impeding the gravitational flow of rainwater, rendering the land unsuitable for cultivation or construction. Adding commercial value to these kaolin deposits can mitigate this environmental impact. As a value addition, alumina can be extracted from kaolin, and extracted alumina can be used as a catalyst, catalytic support or an adsorbent. Recent studies have reported the extraction of alumina from kaolin and its application in the adsorption of toxins such as arsenite, fluoride, and phenol from aqueous solutions [14,15,16]. This study aims to extract the alumina from kaolin found in gem mining sites and evaluate the feasibility of utilizing the extracted alumina as an adsorbent.

## **2. MATERIALS AND METHODS**

### **2.1 Materials**

#### **2.1.1 Chemicals**

HCl and NaOH were purchased from Sisco Research Laboratories (Pvt) Ltd., India. Methylene blue powder was purchased from Shanghai Titan Technology Co., Ltd., China. Commercial alumina ( $\gamma$ - $Al_2O_3$  - 99%) was purchased from Saint-Gobain NorPro Corporation., USA.

#### **2.1.2 Instruments**

Laboratory instruments used in this research were., electronic balance (KERN EW 2200-2NM, Germany), analytical balance (Axis AGN220C model, Poland), electric oven (Equitron-Ecogain Series, India), muffle furnace (Biobase, China), pH meter (Eutech PH 700, USA), orbital shaker (Wiggens WS-100D, China), UV-visible spectrophotometer (Cary 60 Agilent Technologies, Germany), X-Ray Fluorescence spectrometer (HORIBA Scientific XGT - 5200 X-ray, Japan) at SLINTECH, X-Ray Diffractometer (RegakuUltima IV, Japan) at University of Sri Jayewardenepura, X-Ray Diffractometer (Bruker D8 advance, Germany) at University of Moratuwa, Fourier Transform Infrared spectrometer (PerkinElmer, USA) at University of Kelaniya, Scanning Electron Microscope (Zeiss EVO18, Germany) at University of Moratuwa.

### **2.2 Methods**

#### **2.2.1 Sample collection**

Kaolin samples were collected from a gem mining site in Ratnapura District, about 4.5 km southwest of Ratnapura Town, within coordinates 6°40'02.1"N 80°22'44.8"E. The collected samples were stored in zip-lock bags and carefully transported to the laboratory.

#### **2.2.2 Grinding and Sieving**

Kaolin samples were ground using a motor and pestle and then sieved through a 500  $\mu$ m sieve.

#### **2.2.3 calcination**

About 20 g of kaolin samples were measured using an electronic balance and then transferred into a porcelain crucible. Kaolin samples were calcinated in the muffle furnace at 600 °C for 2 hours. After calcination, the weights of the samples were recorded using the same electronic balance.

#### **2.2.4 Acid leaching of alumina**

Alumina was extracted using a 6 M HCl solution as the leaching agent. About 10 g of calcined kaolin was added into 100 mL of the leaching agent, which was previously heated to 90 °C in a 250 mL round flask with condenser. Then, the mixture was stirred at 500 rpm for 2 hours at 90 °C. The resulting slurry was diluted with 100 mL of distilled water and filtered using a Buchner funnel. The filtrate was heated to near boiling, and then an excess volume of 5M NaOH was added to convert alumina into NaAlO<sub>2</sub>. The residue was removed through filtration, and 6M HCl was added to the solution to adjust the pH to 7. Precipitated Al(OH)<sub>3</sub> was filtered, washed with distilled water, and dried at 100 °C in the electric oven for 2 hours. The precipitated Al(OH)<sub>3</sub> was transformed into alumina by calcination in the muffle furnace at 600 °C for 2 hours.

### **2.2.5 Adsorption study**

Extracted and commercial alumina samples were ground using a motor and pestle and sieved through a 500 µm sieve. The methylene blue (MB) stock solution (1000 mg/L) was prepared by dissolving the required quantity of dye in the exact 1 L volume of distilled water. HCl and NaOH solution (0.1 M) was used to adjust the pH of the solution.

MB adsorption onto extracted and commercial alumina was examined under different parameters, including initial dye concentration (1mg/L – 10 mg/L), adsorbent dose (0.200 g – 1.000 g), pH (2-10) and contact time (30 min – 150 min). The suspensions were incubated in an orbital shaker at 120 rpm and filtered through nylon syringe filters (0.45 µm). Then, absorbance (665 nm) was measured using a UV-visible spectrophotometer.

The adsorption capacity was calculated using the equation below, where Co is the initial MB concentration, Ce is the MB concentration at the equilibrium, m is the mass of the adsorbent, and V is the volume of the MB solution.

$$\text{Adsorption Capacity (mg/g)} = \frac{(C_o - C_e)V}{m}$$

### **2.2.6 Characterization**

The chemical composition of kaolin and extracted alumina samples was determined using XRF analysis. The mineralogical identification of kaolin and calcinated kaolin was carried out using XRD analysis. The polymorphic phase of the extracted alumina was identified by using XRD analysis. FTIR analysis was conducted to determine the functional groups of commercial and extracted alumina. Surface characteristics of commercial and extracted alumina were analyzed using a scanning electron microscope.

## **3. RESULTS AND DISCUSSION**

The chemical composition of kaolin was determined via XRF analysis, as shown in Table .1. The kaolin was mainly composed of 63.63 wt% silica and 29.11 wt% alumina. The silica to alumina ratio was 2.18 in the sample. Generally, the silica/alumina ratio in kaolinite mineral is 1.178 [4]. The high silica content in the sample indicates the existence of unbound silica in the form of quartz [4]. Although the kaolin sample contains nearly 30% of alumina, it is considered an economical percentage for the extraction of alumina [12]. Other oxides detected in the XRF analysis were impurities, as they were unrelated to the kaolinite structure. Accordingly, K<sub>2</sub>O, SO<sub>3</sub>, and Fe<sub>2</sub>O<sub>3</sub> were found in amounts exceeding 1% wt, serving as the major impurities.

**Table .1 Chemical composition of kaolin**

<b>Oxide</b>	<b>Average weight (%)</b>
Al <sub>2</sub> O <sub>3</sub>	29.11
SiO <sub>2</sub>	63.63
SO <sub>3</sub>	2.18
K <sub>2</sub> O	1.49
CaO	0.99
TiO <sub>2</sub>	0.10
Fe <sub>2</sub> O <sub>3</sub>	2.08
NiO	0.01
ZnO	0.01
Ga <sub>2</sub> O <sub>3</sub>	0.01
As <sub>2</sub> O <sub>3</sub>	0.01
Rb <sub>2</sub> O	0.01
SrO	0.07
BaO	0.05
Nd <sub>2</sub> O <sub>3</sub>	0.26

The mineralogical analysis of kaolin and calcined kaolin was performed using XRD, as shown in Figure 1 and Figure 2, respectively. The XRD spectrum of kaolin shows the characteristic peaks of kaolinite. Kaolin is a layered silicate consisting of alumina octahedral and silica tetrahedral sheets [17]. Strong ionocovalent bonds are between the alumina and silica sheets [17]. These bonds prevent the dissolution of aluminum ions under low temperatures and short retention in the leaching process [18]. Kaolin was calcinated at a temperature of 500 °C - 900 °C to transform into the amorphous metakaolin phase, facilitating the extraction of aluminum ions [12]. In previous studies, calcination temperature was typically between 700 °C - 800 °C [10,11,13]. High calcination temperatures are associated with high energy consumption and carbon footprint [17]. However, kaolin requires temperatures above 575 °C to transform into metakaolin by removing its structural water [8]. In this study, kaolin was calcined at 600 °C, setting the calcination temperature at the lowest. The XRD analysis of calcined kaolin (Figure .2) shows the irregular bands that confirmed the transformation of the kaolin into the amorphous metakaolin phase.

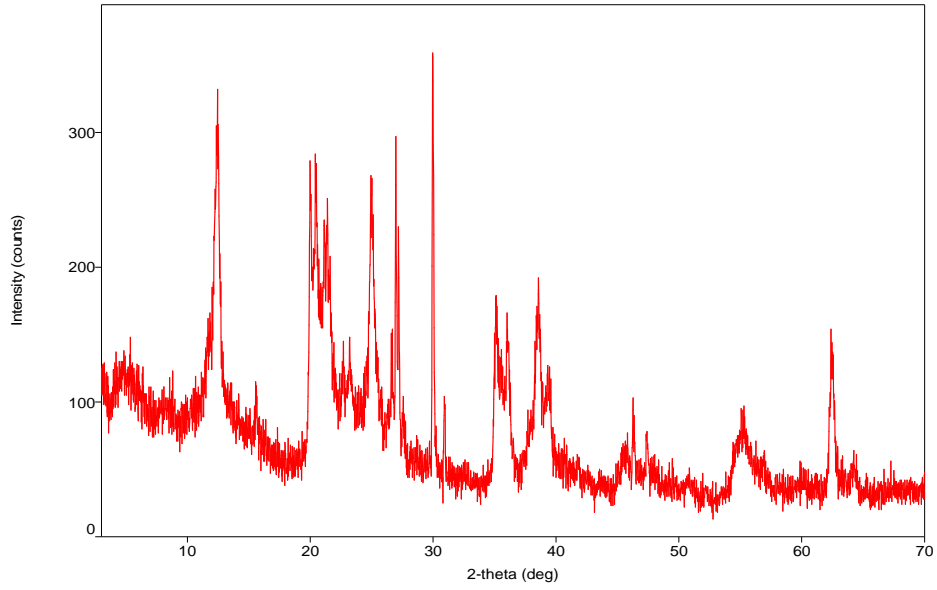


**Figure 1. XRD spectrum of kaolin**

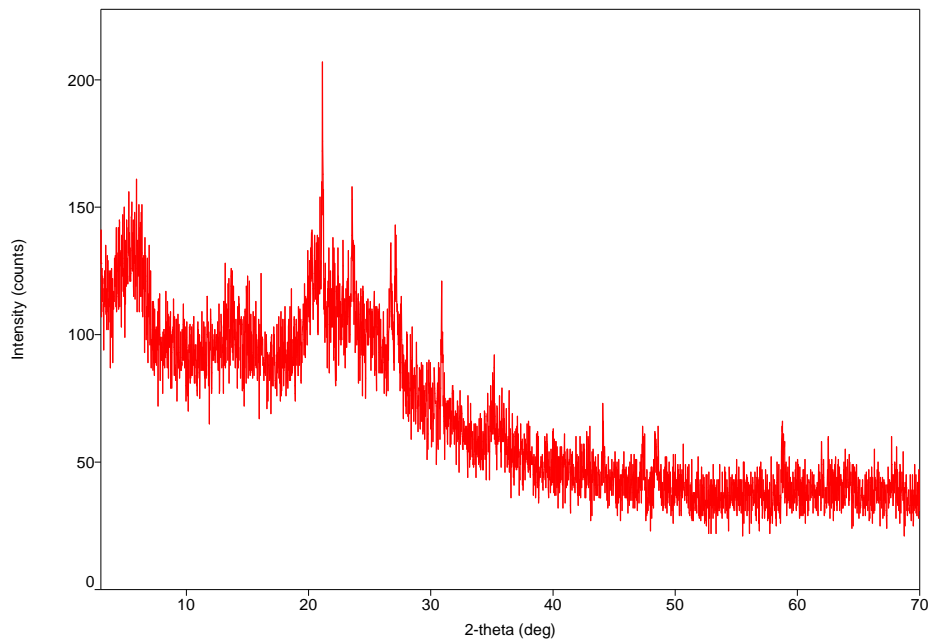


**Figure 2. XRD spectrum of calcined kaolin**

The XRF analysis (Table 2) reveals the chemical composition of the extracted alumina. Alumina was the major element, accounting for 90.03 wt%, and the silica content was 6.64% wt. The silica to

alumina ratio was reduced to 0.07, indicating the effective removal of silica through the extraction process. The metal impurities were recorded at less than 1 wt% in the extracted alumina, indicating the effective removal of metal impurities by the extraction process.

**Table 2: Chemical composition of extracted alumina**

Oxide	Average weight (%)
Al <sub>2</sub> O <sub>3</sub>	90.03
SiO <sub>2</sub>	6.64
P <sub>2</sub> O <sub>5</sub>	2.14
SO <sub>3</sub>	0.20
K <sub>2</sub> O	0.07
CaO	0.69
V <sub>2</sub> O <sub>5</sub>	0.01
Fe <sub>2</sub> O <sub>3</sub>	0.08
CuO	0.03
ZnO	0.08
Ga <sub>2</sub> O <sub>3</sub>	0.04

The crystalline phase of the extracted alumina was identified through XRD analysis (Figure 3). The characteristic peaks of  $\gamma$ -alumina at  $2\theta$  angles of  $45.90^\circ$  and  $66.92^\circ$  were observable in the resulting XRD pattern [2,12]. The thermal stability of  $\gamma$ -alumina was significantly improved in the presence of some materials, including CaO, TiO<sub>2</sub>, and SiO<sub>2</sub> [19]. Silicon was found to be the most effective element in stabilizing alumina, and it notably retarded the transformation of  $\gamma$ -alumina into  $\alpha$ -alumina [20]. XRF analysis (Table .2) revealed the presence of SiO<sub>2</sub> and CaO in the extracted alumina, which may aid in stabilizing alumina as the  $\gamma$ -phase.

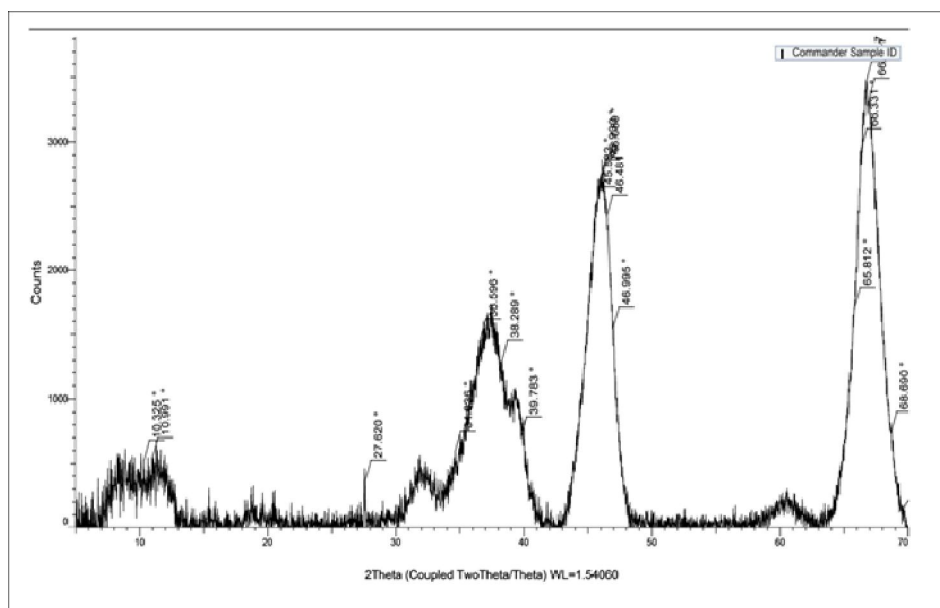


**Figure .3.XRD spectrum of extracted alumina**

The functional groups in commercial and extracted alumina samples were identified through FTIR analysis, shown in Figures .4 and .5. The strong broadening band from  $3700\text{ cm}^{-1}$  to  $3000\text{ cm}^{-1}$  in both spectra indicated the hydrogen bonds between various hydroxyl groups in the alumina [6]. The peak observed at  $1634\text{ cm}^{-1}$  in both spectra represented the stretching vibration of the Al-OH groups [5]. The strong broadening band from  $1000\text{ cm}^{-1}$  to  $500\text{ cm}^{-1}$  in both spectra indicated the  $\gamma$ -alumina phase [5]. According to FTIR analysis, both commercial and extracted alumina contained hydroxyl groups, which enhance the adsorption ability of the  $\gamma$ -alumina phase [6].

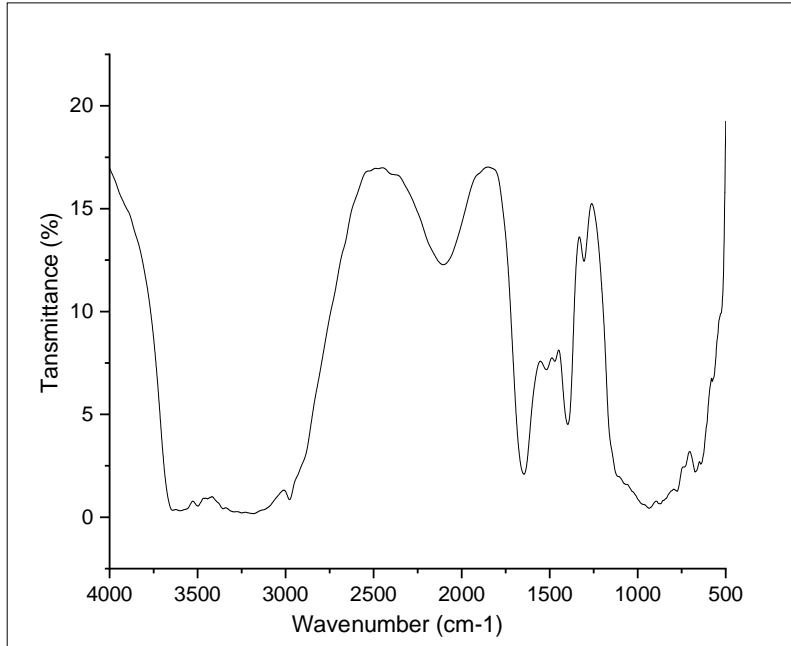


**Figure .4. FTIR spectrum of extracted alumina**

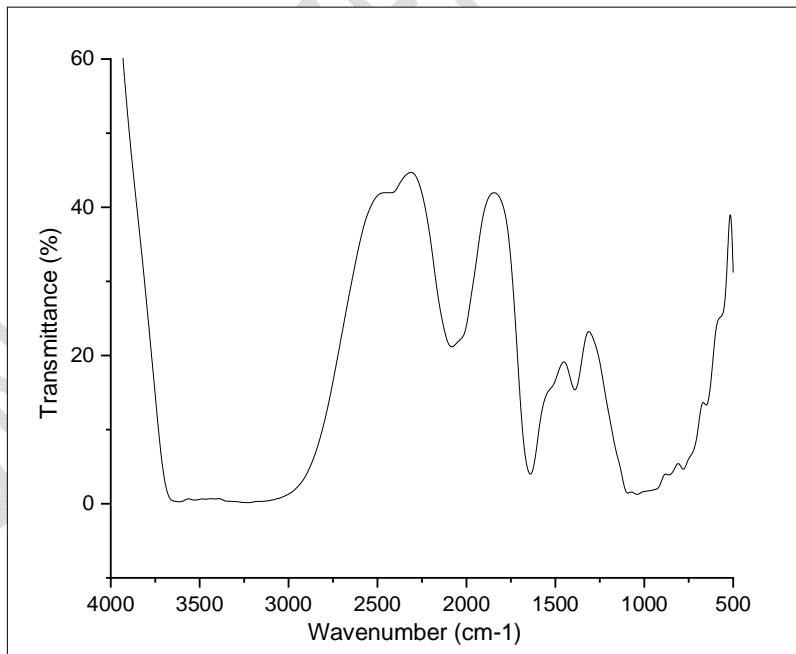
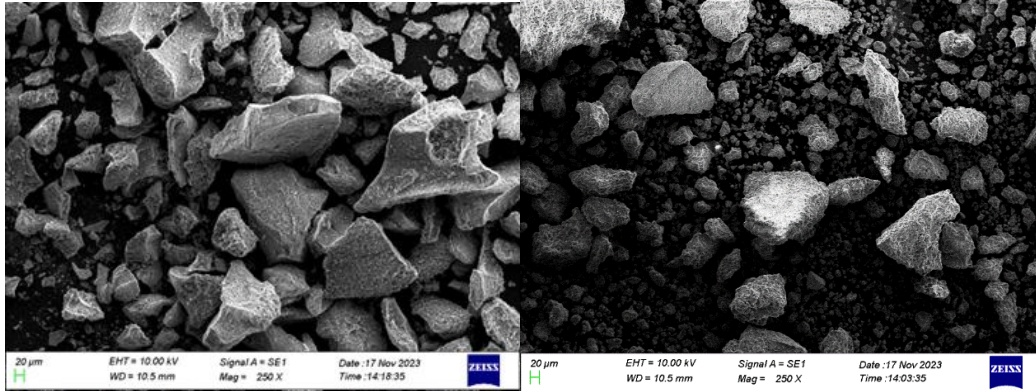


**Figure .5 FTIR spectrum of commercial alumina**

The morphology of the extracted and commercial alumina was examined through SEM analysis. As shown in Figure 6, both alumina particles have irregular and non-uniform shapes with sharp edges. The SEM images (Figure.6 (a),(b)) show that both particles exhibit heterogeneous surfaces with different pore sizes and shapes. According to Figure .6 (c) (d), commercial alumina particles appeared to have a higher surface area than extracted alumina due to their high porosity.

(a),(b).



(c).

(d).

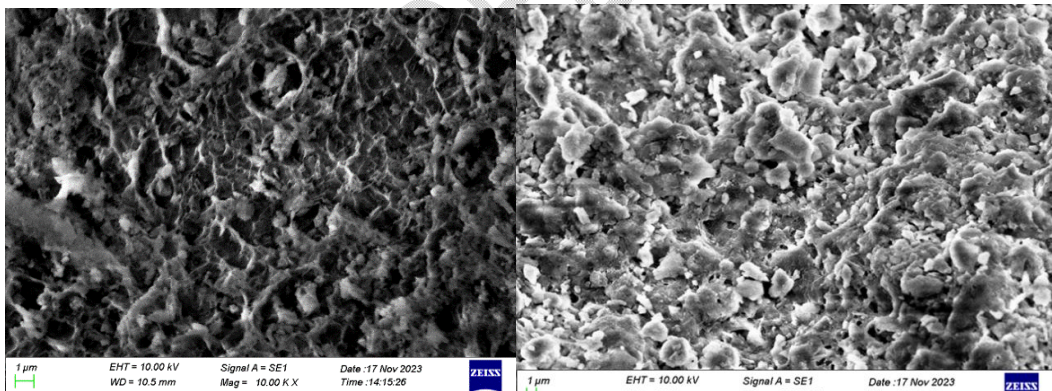


**Figure .6. SEM images of alumina particles  
(a),(c)-Extracted alumina (b),(d)-Commercial alumina**

Figure 7 illustrates the effect of the initial dye concentration on the adsorption capacity of both extracted alumina and commercial alumina. Overall, the adsorption capacity increased as the initial dye concentration increased up to 8 mg/L for both samples. However, the adsorption capacity of both samples slightly decreased as the initial dye concentration increased from 8 mg/L to 10

mg/L. Increasing the dye concentration elevates the abundance of absorbate at the interface [6]. The high abundance of absorbate at the interface increased the chances of collision between the absorbate and the adsorbent surface, causing an increase in adsorption [6]. The slight decrease in adsorption capacity at the highest initial dye concentration occurred due to the absence of a sufficient number of active sites for adsorption [21].

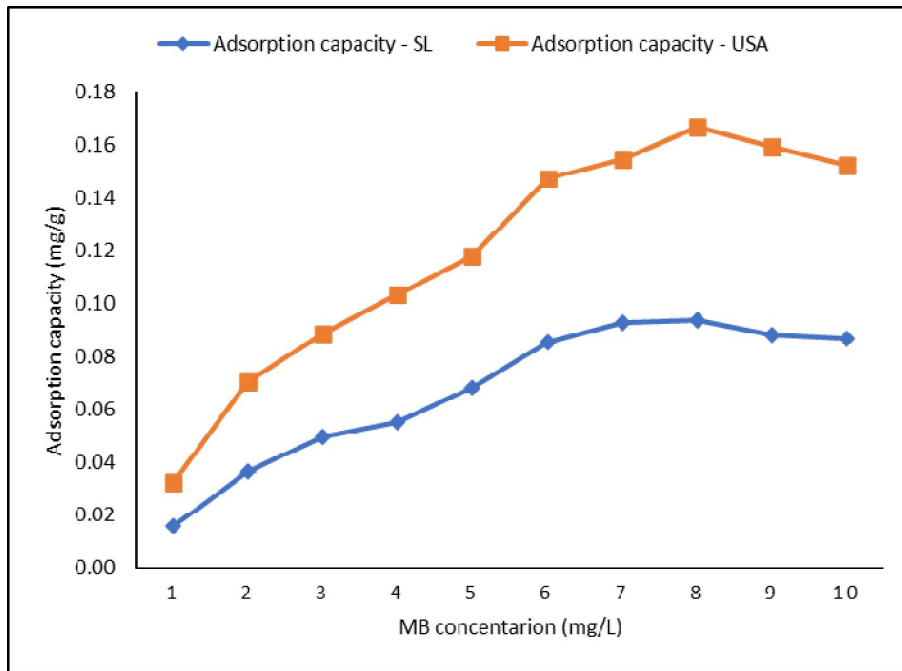


**Figure .7. Effect of initial MB concentration on adsorption capacity**

The effect of the adsorbent dose on adsorption capacity is indicated in Figure .8. According to the graph, the adsorption capacity increased with an increase in adsorbent dose for both commercial and extracted alumina. An increase in adsorbent dose led to a higher availability of active sites for adsorption, resulting in an overall increase in adsorption capacity [22].

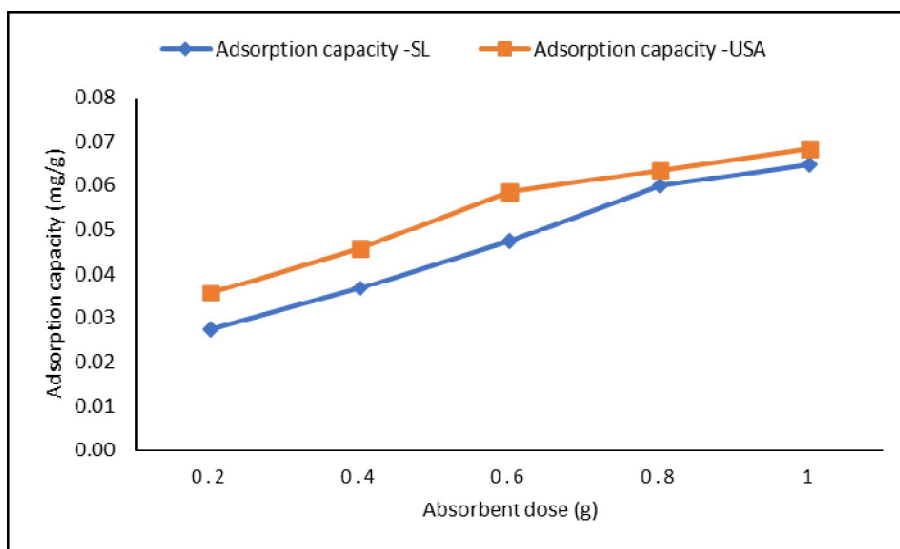


**Figure 8. Effect of adsorbent dose on adsorption capacity**

The adsorption of MB onto commercial alumina and extracted alumina was found to be pH dependent (Figure .9). The overall adsorption capacity of both commercial and extracted alumina increased with an increase in the pH of the solution. At acidic pH, the competition between H<sup>+</sup> ions and the cationic group of MB for adsorption sites causes a reduction in the uptake of MB by the adsorbent [23]. The pK<sub>a</sub> value of MB is 0.04 [24]. Therefore, at alkaline pH, dye molecules get completely dissociated into their ionic form and are strongly attracted to the negatively charged sites of the adsorbent, increasing the adsorption [5]. The extracted alumina exhibited a relatively high adsorption capacity even at low pH. This phenomenon may be attributed to isomorphous substitution, which is pH independent [25]. The extracted alumina contains several metal impurities that can be exchanged with cationic MB molecules.

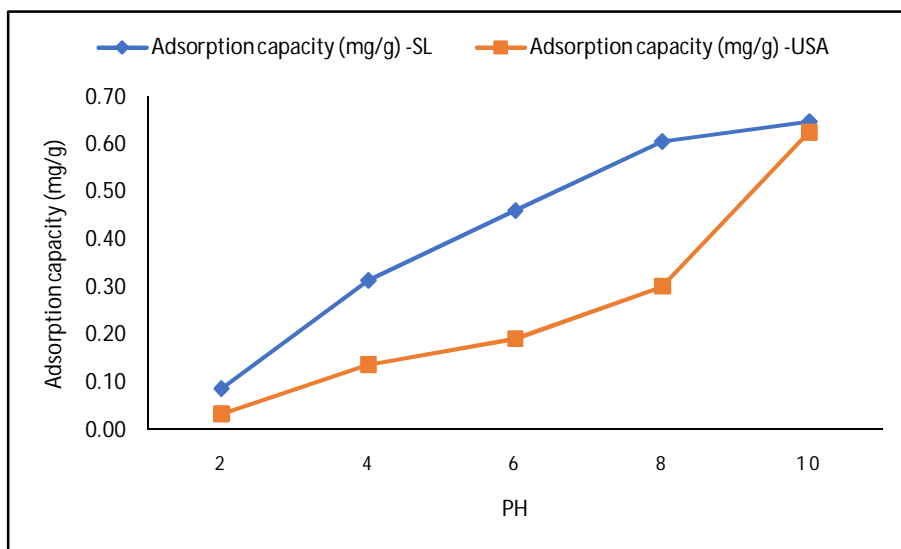


**Figure 9. Effect of pH on adsorption capacity**

Figure .10 illustrates the effect of contact time on adsorption capacity. The adsorption capacity of commercial and extracted alumina increased until the contact time reached 120 minutes. Further increasing the contact time did not cause an increase in the adsorption. Increasing the contact time allowed more collision between adsorbate and adsorbent, leading to increased adsorption; this continued until the saturation of adsorption sites with dye molecules [26]. After the saturation, further increasing the contact time did not affect adsorption [26].

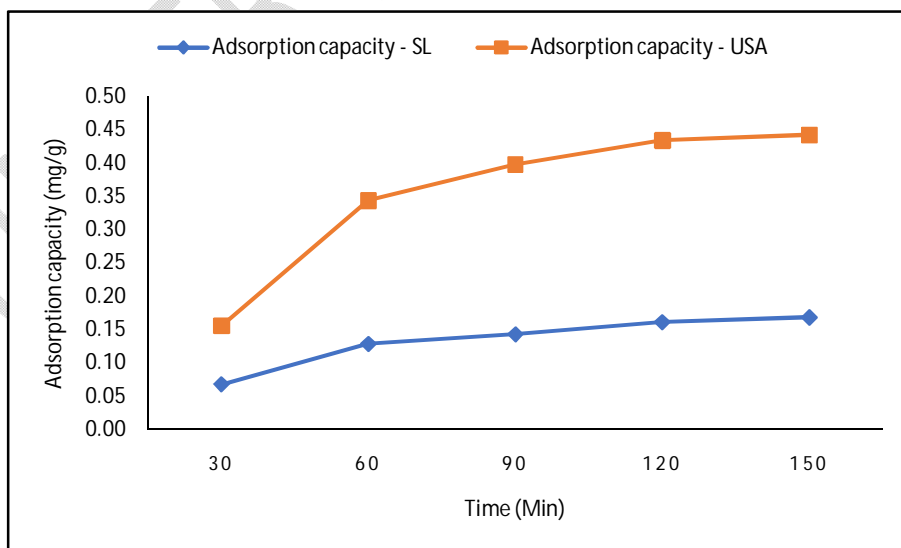


**Figure .10. Effect of contact time on adsorption capacity**

In this study, commercial and extracted alumina exhibited the same trend toward the adsorption parameters (initial dye concentration, adsorbent dosage, pH, and contact time). However, in most cases, the adsorption capacity of the commercial alumina was recorded as higher than that of the extracted alumina. The higher adsorption capacity of the commercial alumina may be attributed to its high purity (99%  $\gamma$ -alumina) and the high surface area.

## CONCLUSION

Kaolinitic clay found at gem mining sites contains approximately 29% alumina by weight. Alumina was extracted by calcining the kaolin at 600°C, followed by acid leaching using 6M HCl as the leaching agent and 5M NaOH as the precipitating agent. The extracted alumina had a purity exceeding 90% and was in the  $\gamma$ -phase. The extracted alumina exhibited adsorption characteristics comparable to those of commercial alumina in the adsorption of methylene blue. High-purity alumina can be produced from the kaolinitic clay found at gem mining sites, and the extracted alumina has potential applications as an adsorbent.

Disclaimer (Artificial intelligence)

Option 1:

Author(s) hereby declare that NO generative AI technologies such as Large Language Models (ChatGPT, COPILOT, etc) and text-to-image generators have been used during writing or editing of manuscripts.

Option 2:

Author(s) hereby declare that generative AI technologies such as Large Language Models, etc have been used during writing or editing of manuscripts. This explanation will include the name, version, model, and source of the generative AI technology and as well as all input prompts provided to the generative AI technology

Details of the AI usage are given below:

- 1.
- 2.
- 3.

## REFERENCES

1. Yang, H., Liu, M., & Ouyang, J. Novel synthesis and characterization of nanosized  $\gamma$  Al<sub>2</sub>O<sub>3</sub> from kaolin. *Applied Clay Science*.2010;47(3-4):438-443.<https://doi.org/10.1016/j.clay.2009.12.021>
2. Salahudeen, N., Ahmed, A. S., Al-Muhtaseb, A. H., Dauda, M., Waziri, S. M., & Jibril, B. Y. Synthesis of gamma alumina from Kankara kaolin using a novel technique. *Applied Clay Science*.2015;105:170–177.<https://doi.org/10.1016/j.clay.2014.11.041>
3. Abdou, N. Y., Sabry, M., & El-Faramawy, N. Thermoluminescence characteristics of different phase transitions from nanocrystalline alumina. *Journal of Radioanalytical and Nuclear Chemistry*. 2022; 331(9):3865–3876. <https://doi.org/10.1007/s10967-022-08437-4>
4. Ibrahim, K. M., Moumani, M. K., & Mohammad, S. K. Extraction of  $\gamma$ -alumina from low-cost kaolin. *Resources*.2018;7(4):63. <https://doi.org/10.3390/resources7040063>
5. Banerjee, S., Gautam, R. K., Jaiswal, A., Chattopadhyaya, M. C., & Sharma, Y. C. Rapid scavenging of methylene blue dye from a liquid phase by adsorption on alumina nanoparticles. *RSC Advance*. 2015; 5(19):14425–14440.
6. Sangor, F. I. M. S., & Al-Ghouti, M. A. Waste-to-value: Synthesis of nano-aluminum oxide (nano- $\gamma$ -Al<sub>2</sub>O<sub>3</sub>) from waste aluminum foils for efficient adsorption of methylene blue dye. *Case Studies in Chemical and Environmental Engineering*. 2023;8:100394. <https://doi.org/10.1016/j.cscee.2023.100394>
7. Pak, V. I., Kirov, S. S., Nalivaiko, A. Yu., Ozherelkov, D. Yu., & Gromov, A. A. Obtaining Alumina from Kaolin Clay via Aluminum Chloride. *Materials*.2019;12(23):3938. <https://doi.org/10.3390/ma12233938>
8. Ali, A., AL-Taie, M., & Ayoob, I. The Extraction of Alumina from Kaolin. *Engineering and Technology Journal*. 2019;37(4A):133–139. <https://doi.org/10.30684/etj.37.4a.4>
9. Al-Ajeel, A. W. A., & Suad, I. A.S. Alumina recovery from Iraqi kaolinitic clay by hydrochloric acid route. *Iraqi Bulletin of Geology and Mining*.2006;2(1):67-76.
10. Bagherzadeh, Y., Golmakani, M. H., & Karimi, E. Z. Straight Synthesis of  $\alpha$  and  $\gamma$  Alumina from Kaolin by HCl Acid Leaching. *Journal of Mining and Metallurgy*. 2023;17-27.
11. Hosseini, S. A., Niaei, A., & Salari, D. Production of  $\gamma$ -Alumina from Kaolin. *Open Journal of Physical Chemistry*.2011;01(02):23-27. <https://doi.org/10.4236/ojpc.2011.12004>

12. ElDeeb, A. B., Brichkin, V. N., Kurtenkov, R. V., & Bormotov, I. S. Extraction of alumina from kaolin by a combination of pyro- and hydro-metallurgical processes. *Applied Clay Science*. 2019;172:146–154. <https://doi.org/10.1016/j.clay.2019.03.008>
13. Bhattacharyya, S., & Behera, P. S. Synthesis and characterization of nano-sized  $\alpha$ -alumina powder from kaolin by acid leaching process. *Applied Clay Science*. 2017;146:286-290. <https://doi.org/10.1016/j.clay.2017.06.017>
14. KhodadadiDarban, A., Kianinia, Y. and Taheri-Nassaj, E. Synthesis of nano-alumina powder from impure kaolin and its application for arsenite removal from aqueous solutions. *Journal of Environmental Health Science and Engineering*. 2013;11:1-11. <https://doi.org/10.1186/2052336x-11-19>
15. Yadav, A.K. and Bhattacharyya, S. Preparation of porous alumina adsorbent from kaolin using acid leach method: studies on removal of fluoride toxic ions from an aqueous system. *Adsorption*. 2020;26(7):1073-1082. <https://doi.org/10.1007/s10450-019-00193-4>
16. Salahudeen, N., Ahmed, A.S., Ala'a, H., Dauda, M., Waziri, S.M., Jibril, B.Y. and Al-Sabahi, J. Synthesis, characterization and adsorption study of nano-sized activated alumina synthesized from kaolin using novel method. *Powder Technology*. 2015;280:266-272. <https://doi.org/10.1016/j.powtec.2015.04.024>
17. Maria, B., Efthymios, B., & Dimitrios, P. Exploitation of Kaolin as an Alternative Source in Alumina Production. *Material Proceedings*. 2021;5(1):24. <https://doi.org/10.3390/materproc2021005024>
18. Tantawy, M. A., & Ali Alomari, A. Extraction of Alumina from Nawan Kaolin by Acid Leaching. *Oriental Journal of Chemistry*. 2019;35(3):1013–1021. <https://doi.org/10.13005/ojc/350313>
19. Belver, C., Banares Munoz, M. A., & Vicente, M. A. Chemical activation of a kaolinite under acid and alkaline conditions. *Chemistry of Materials*. 2002;14(5):2033–2043. <https://doi.org/10.1021/cm0111736>
20. Liu, Q., Wang, A., Wang, X., Gao, P., Wang, X., & Zhang, T. Synthesis, characterization and catalytic applications of mesoporous  $\gamma$ -alumina from boehmite sol. *Microporous and Mesoporous Materials*. 2008;111(1–3):323–333. <https://doi.org/10.1016/j.micromeso.2007.08.007>
21. Ebadollahzadeh, H., & Zabihi, M. Competitive adsorption of methylene blue and Pb (II) ions on the nano-magnetic activated carbon and alumina. *Materials Chemistry and Physics*. 2020;248:122893. <https://doi.org/10.1016/j.matchemphys.2020.122893>
22. Raut, P. A., Dutta, M., Sengupta, S., & Basu, J. K. Alumina-carbon composite as an effective adsorbent for removal of Methylene Blue and Alizarin Red-s from aqueous solution. *Indian Journal of Chemical Technology*. 2013;20:15–20.
23. Adesina, A. O., Elvis, O. A., Mohallem, N. D. S., & Olusegun, S. J. Adsorption of Methylene blue and Congo red from aqueous solution using synthesized alumina–zirconia composite. *Environmental Technology (United Kingdom)*. 2021;42(7):1061–1070. <https://doi.org/10.1080/09593330.2019.1652696>
24. Chowdhury, S., & Saha, P. Das. Biosorption of methylene blue from aqueous solutions by a waste biomaterial: Hen feathers. *Applied Water Science*. 2012;2(3):209–219. <https://doi.org/10.1007/s13201-012-0039-0>

25. Ferrero, F. Adsorption of Methylene Blue on magnesium silicate: Kinetics, equilibria and comparison with other adsorbents. *Journal of Environmental Sciences*. 2010;22(3):467-473. [https://doi.org/10.1016/S1001-0742\(09\)60131-5](https://doi.org/10.1016/S1001-0742(09)60131-5)
26. Hariani, P. L., Muryati, & Fatma, F. Synthesis Alumina-Activated Carbon Composite Using Sol-Gel Method As Adsorption for Methylene Blue Dye. *Journal of Physics: Conference Series*. 2018;1095(1):012026. <https://doi.org/10.1088/1742-6596/1095/1/012026>

UNDER PEER REVIEW